Acta Polytechnica CTU Proceedings **36**:253–260, 2022
https://doi.org/10.14311/APP.2022.36.0253

Published by the Czech Technical University in Prague

SIMPLIFIED MODELLING OF THE PERFORMANCE OF CONCRETE TUNNELS DURING FIRE AND POST-FIRE DAMAGE CLASSIFICATION

Ruben Van Coile[a,*], Balša Jovanović[a], Ranjit Kumar Chaudhary[a], Xavier Deckers[b], Andrea Lucherini[a]

[a] *Ghent University, Department of Structural Engineering and Building Materials, Technologiepark-Zwijnaarde 60, 9052 Gent, Belgium*

[b] *Fire Engineered Solutions Ghent - A Jensen Hughes Company, Oudenaardsesteenweg 32 G, 9000 Ghent, Belgium*

[*] corresponding author: Ruben.VanCoile@ugent.be

Abstract. The performance of concrete tunnel structures during and after fire is not well understood. This is an obstacle to the adoption of risk-based approaches for fire safety design of tunnel structures. Upon the request of the Belgian fire safety consultancy FESG, a simplified assessment of the collapse probability and post-fire damages for a reference tunnel structure has been made. The structural system is modelled through 2D beam finite elements, where spalling rates have been assumed based on available literature data. Structural stability is verified for both the heating and cooling phases of the fire. In those cases where the structure survives up to burnout, the residual deformations and thermal damage to the tunnel structure are assessed.

Keywords: Damage, failure probability, fire, spalling, tunnel.

1. Introduction

The structural fire design of concrete road tunnels is commonly done with reference to prescriptive guidance and regulations. The actual performance achieved in case of a fire is not well understood, both in terms of the probability of failure (collapse during fire), as well as the probability density function of the damage post-fire (permanent damage and residual deflections, repair costs). This hampers the adoption of risk-based approaches to the fire safety design of road tunnels, and is an obstacle for risk-based code-calibration.

The Belgian fire engineering consultancy FESG has been developing a simplified risk assessment tool for tunnel structures. This risk assessment requires an evaluation of the probability of structural failure during fire and of the extent of the post-fire damage and downtime. This will allow for the comparison of design alternatives, e.g. with respect to active and passive fire safety measures. For further details on the project and a conceptual framework for decision making for tunnel fire safety, see [1].

In cooperation with FESG, a simplified assessment of the performance of a reference concrete tunnel structure during and after fire has been made. A 2D beam finite element model is adopted, taking into account the effect of concrete spalling through nominal spalling rates. The fire is modelled through a heating phase according to the nominal RWS curve, followed by a decay phase based on limited experimental data. Details of the approach and key outcomes are provided in the following.

2. Modelling approach

2.1. Reference tunnel section

The reference tunnel cross section is visualized in Figure 1, with tunnel lining cross-sectional characteristics (per unit length) listed in Table 1. The cross-section is inspired by an existing design consisting of two one-directional tubes and a central connecting tube for evacuation purposes and maintenance. For simplicity (calculation time), all walls are identical and no reinforcement curtailment has been modelled. Soil resistance to outwards movement of the tunnel is modelled through springs. A structural mesh of 0.5 m is applied. A fine thermal mesh is applied (5 to 10 mm element width perpendicular to the heat transfer direction). The structural modelling is done using SAFIR [2].

Other input parameters for the analysis (material and mechanical properties of concrete and reinforcement) are listed in Table 2. The adopted concrete model is an extension to the EN 1992-1-2:2004 [3] model, taking into account explicit modelling of transient creep [4]. Concrete tensile strength is neglected. The concrete compressive strength and reinforcement yield strength are considered in the model with their expected values. This is the preferred approach for implementation in the larger risk-based framework. Furthermore, due to the complex structural behaviour of the tunnel system, it is not a priori clear if a larger or smaller value of the material strength and stiffness is "more conservative". The concrete Poisson coefficient is an artefact from model development. A lower temperature-dependent Poisson coefficient can

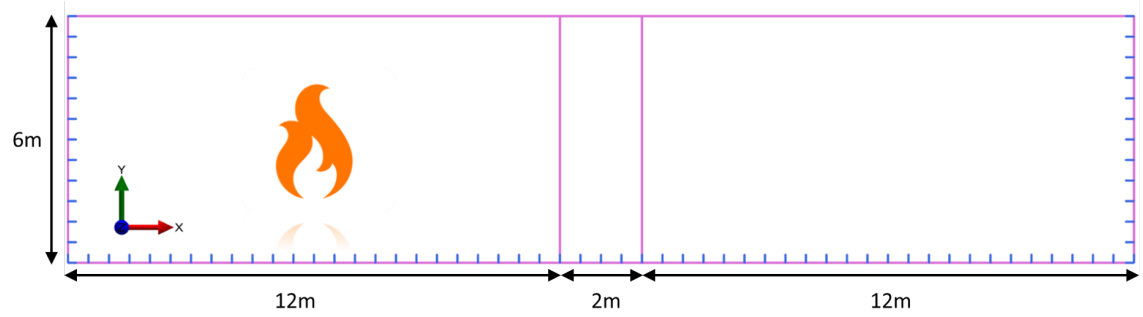

Figure 1. Section of the reference tunnel and dimensions (lining axis positions). The blue lines are springs modelling the soil interaction.

Parameter	Ceiling and floor	Walls
Thickness [mm]	600	410
Concrete cover [mm]	70	100
Reinforcement axis distance to concrete surface [mm]	75	105
Reinforcement area (single layer) [mm^2]	5300 $\varnothing 25-100$	2010 $\varnothing 16-100$

Table 1. Tunnel cross-sectional characteristics (per unit length).

be recommended, in accordance with [5].

Parameter	Value
Concrete compressive strength [MPa]	42
Concrete tensile strength [MPa]	0
Concrete Poisson coefficient [−]	0.3
Reinforcement yield strength [MPa]	560
Reinforcement initial modulus of elasticity [GPa]	210
Reinforcement Poisson coefficient [−]	0.3

Table 2. Material parameters.

Upon cooling, concrete loses an additional 10% of strength in accordance with EN 1994-1-2:2005 recommendations. The reinforcement fully recovers upon cooling. The latter is a simplification that overestimates reversibility for reinforcement which has exceeded 600°C [6]. This simplification is in line with the state-of-the-art, but means that cooling results for reinforcement that has exceeded 600°C need to be interpreted with care. Fundamental research is needed to develop a model for the material behaviour during the cooling phase.

The tunnel is loaded with 1 m of soil (weight 17.5 kN/m^3) and 2 kN/m^2 permanent load at ground level. The lateral earth pressure coefficient is set at 0.4. The tunnel is considered to be above the ground water table (no upwards water pressure). These values were chosen to represent a city tunnel for through traffic. A characteristic imposed load of 30 kN/m^2 is considered. The mean imposed load is assessed as 0.2 times the characteristic value, in analogy with building design [7]. Improved live load modelling for geotechnical structures, and the consideration of the local geotechnical parameters are recommended.

2.2. Fire exposure

As the tunnel is symmetrical, fire is considered in one of the road tubes only (see Figure 1). The likelihood independent simultaneous occurrence of fire in both tubes is considered negligible. Within the larger risk assessment tool, a detailed assessment of fire severity is made, taking into account fire spread and the interaction with active fire safety measures. For the structural performance evaluation, these fire severities are mapped onto an equivalent heating duration for the nominal RWS fire curve [8]. The following nominal durations are considered: 15/30/60/120/180 min.

The fire exposure is applied to the walls and ceiling, considering a convective heat transfer coefficient of 50 W/(m^{2}K) and emissivity of 0.7, based on EN 1992-1-2:2004 [3]. The decay phase is modelled through Equation 1, with θ_c, θ_{ref} and θ_{max} respectively the fire curve temperature in the cooling phase, the reference ambient temperature (20°C) and the maximum RWS fire temperature during the heating phase. The time in minutes since the nominal start of the fire and the time of heating phase duration are denoted by t and t_{max}, while the speed of the decay is governed by the decay parameter b. To evaluate the decay parameter b in Equation 1, the decay phases of 19 test measurements were extracted from [9]. An average value of 0.025 min^{-1} was estimated and adopted (mean value preferred for cost-benefit evaluations in a later stage). For concrete structures, the cooling phase behaviour is of great importance, both due to the delayed heating of the cross-section, as well as

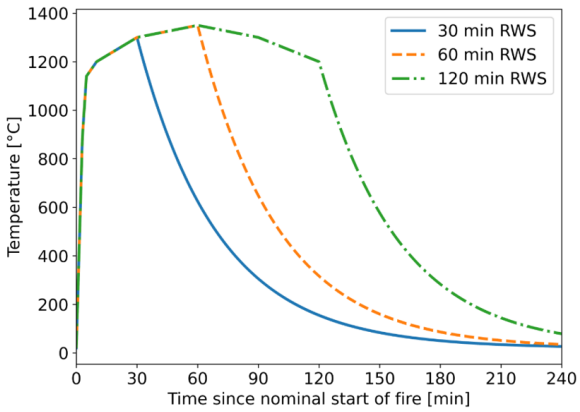

FIGURE 2. Example fire curves. RWS heating phase and exponential decay phase. Temperatures to be interpreted as adiabatic surface temperatures.

due to the fire-induced permanent deformations resulting in a possible force redistribution. The obtained temperature-time curves are visualized in Figure 2.

$$\theta_c - \theta_{ref} = (\theta_{max} - \theta_{ref})\, e^{-b(t-t_{max})} \qquad (1)$$

2.3. Concrete spalling

Spalling is modelled considering nominal spalling rates, as recommended in [10] and applied by [11]. Specifically, the start of spalling is fixed at 1 min after the nominal start of the exposure, followed by a constant spalling rate of, for example, 3 mm per minute. Spalling is stopped as soon as either (i) the reinforcement layer is reached, or (ii) when the fire enters the decay phase. The spalling is implemented in SAFIR through an automated procedure, as described in [11].

Considering the current state-of-knowledge, it is recommendable to consider all unprotected concrete to be prone to spalling. Earlier definitions of spalling-free concrete mixes have later been shown susceptible to spalling after all, see e.g. [12]. Especially in the case of severe fire exposures as adopted for tunnels, (limited) spalling of unprotected concrete can be assumed. The addition of polypropylene fibres is considered to reduce the concrete propensity to spall [13]. Most literature sources ascribe this to an increased porosity (and thus the reduction in pore pressures) during fire. Concrete with polypropylene fibres is assigned a spalling probability of 40%. This number is based on a study of spalling occurrence in an unpublished test campaign and should be considered as engineering judgement. For protected concrete, spalling is considered not to occur. This does not imply that local spalling is deemed impossible in case of protected concrete. The occurrence of spalling across the entire exposed surface is however deemed very unlikely.

Hua et al. [11] report spalling rates for tunnels of up to 5 mm/min. In the current study nominal spalling rates of 1/2/3/3.75/5 mm/min are considered, as well as a no-spalling case. The spalling severity

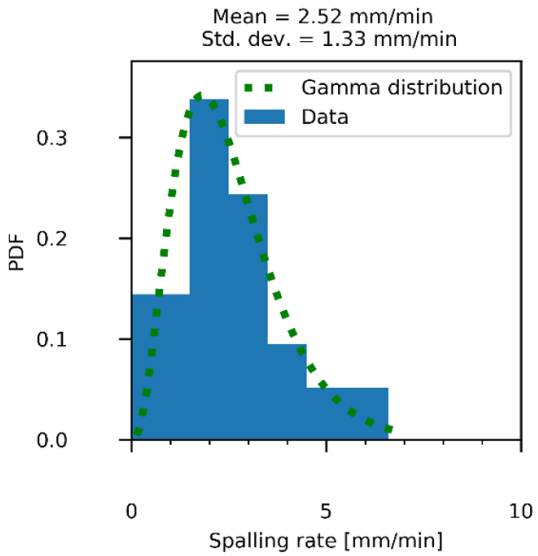

FIGURE 3. Spalling rate data listed by Hua et al. (2021) and fitted Gamma distribution.

Spalling rate [mm/min]	Probability
1.00	0.091
2.00	0.313
3.00	0.292
3.75	0.139
5.00	0.165

TABLE 3. Assessment of conditional probabilities for the spalling severity.

probabilities (conditional probability given spalling) are derived from the data listed by [11]. A theoretical distribution describing the spalling rate probability density is fitted on the data whereby each literature data point is treated equally. Applying the Akaike Information Criterion (AIC) [14], a Gamma distribution (Equation 2, with Γ the gamma function, and x the spalling rate) with shape factor $k = 3.6$ and scale factor θ =0.7 is chosen as the best fit (see obtained fit in Figure 3). Based on this distribution, probabilities for each spalling rate used in this study are calculated and presented in Table 3. These probabilities have been calculated considering the nominal spalling rates as upper bounds for their respective interval (with the exception of the highest nominal spalling rate of 5 mm/min).

$$f(x) = \frac{1}{\Gamma(k) \cdot \theta^k}\; x^{k-1} e^{(x/\theta)} \qquad (2)$$

2.4. Post-fire damage assessment

Reinforced concrete structures exhibit permanent damage following fire [6]. Concrete exhibits a permanent loss of strength and stiffness following heating to elevated temperatures and subsequent cooling, and also reinforcement exhibits a permanent loss of

Damage states	Thermal damage	Repairability
DS0	D300 $\cong$ 0	No repair required
DS1	0 < D300 < c/10	Clean surface and replace damaged concrete
DS2	c/10 $\leq$ D300 < c	Clean surface and replace damaged concrete
DS3	c $\leq$ D300 < d/4	Clean surface and replace damaged concrete
DS4	d/4 $\leq$ D300 < d/2	Demolish and reconstruct

Table 4. Thermal damage states, with c the concrete cover and d the thickness of the cross-section.

Damage states	Structural damage ceiling	Repairability	Structural damage wall	Repairability
DS0	Δs/l < 1/240	No repair required	Δc/h < 0.5%	No repair required
DS1	1/240 $\leq \Delta s$/l < 1/120	No repair required	Δc/h $\geq$ 0.5%	Demolish and reconstruct
DS2	1/120 $\leq \Delta s$/l < 1/60	Demolish and reconstruct		–
DS3	1/60 $\leq \Delta s$/l	Demolish and reconstruct		

Table 5. Structural damage states, with Δs the mid-span residual vertical displacement, l the ceiling span, Δc the mid-height residual horizontal displacement, and h half of the wall height.

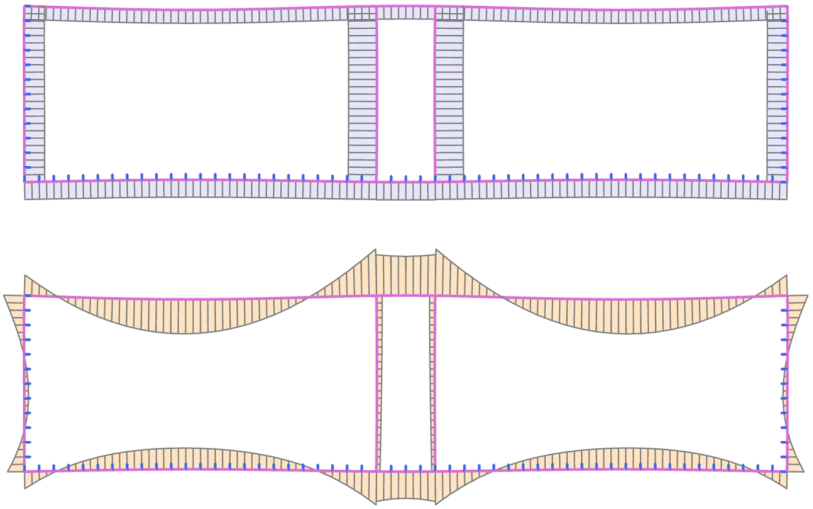

Figure 4. Axial force (top; compression blue) and bending moment (bottom) before the fire.

strength following exposure to temperatures in excess of 600°C [6]. Both these damage effects are on a material level. The fire exposure also results in fire-induced forces (restraining effects), permanent thermal strains, and load redistribution due to changes in stiffness. These effects result in residual deformations post-fire. These residual deformations may jeopardize the serviceability of the tunnel, and also result in second order load effects. These latter damage effects are on a system (structural) level.

The concept to pre-evaluate the repair costs of concrete structures following fire exposure is relatively new. A recent in-depth investigation for concrete structures has been presented in [15]. The evaluation of concrete fire damage through the 300°C isotherm (D300) and residual deformations is recommended. These damage parameters are then used to determine the damage class and repair feasibility. The study by Ni and Gernay also elaborates an approach for repair cost of fire-damaged structures based on the damage states. Specifically, RSMeans data is used to inform the cost evaluations. A similar approach as proposed by Ni and Gernay is adopted in the following to evaluate the damage class and repair cost for fire-damaged tunnel structures.

The same limit states as proposed by [15] are used here to determine the damage of the structure. Table 4 and Table 5 below gives the damage states and repairability limit states for thermal and mechanical damages for concrete structures following a fire event.

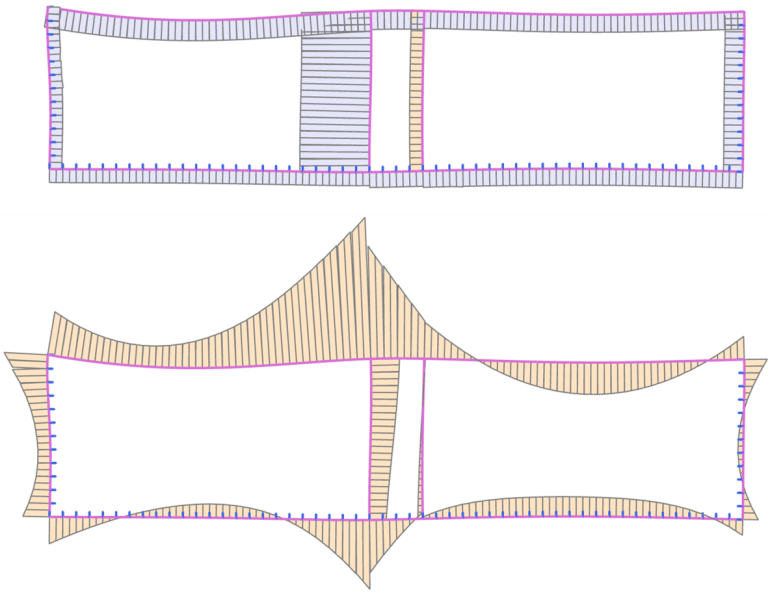

FIGURE 5. Axial force (top; compressive blue) and bending moment (bottom) after approx.. 60 min of fire exposure (beginning of the cooling phase).

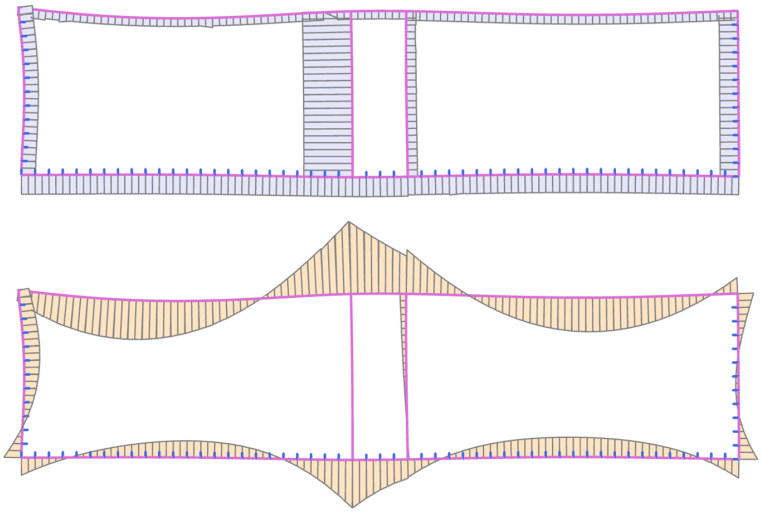

FIGURE 6. Axial force (top; compression blue) and bending moment (bottom) after 12 hours of fire exposure (end of the fire event simulation.

For the damage states of the tunnel ceiling, the damage classification for slabs is adopted, while column limits are adopted for the walls. This is based on the consideration that the tunnel cross-section can be viewed as a 2D frame.

3. RESULTS

3.1. EXAMPLE CASE ANALYSIS - 60 MIN RWS HEATING PHASE, NO SPALLING

In this case study, the walls and ceiling in the left tube are exposed to fire from the interior only. These linings can be considered thermally thick as the cooling conditions on the unexposed side (e.g., adiabatic, or cooling to ambient) do not influence the results. Upon the start of the cooling phase, the hot exposed surface quickly starts to cool as well. The heat wave however

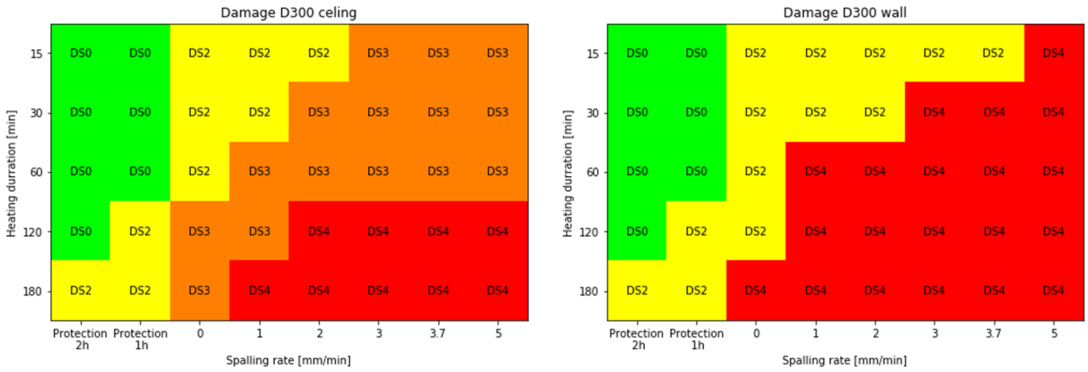

Figure 7. Thermal damage state (ceiling and wall) in function of RWS heating phase duration and nominal rate of concrete spalling.

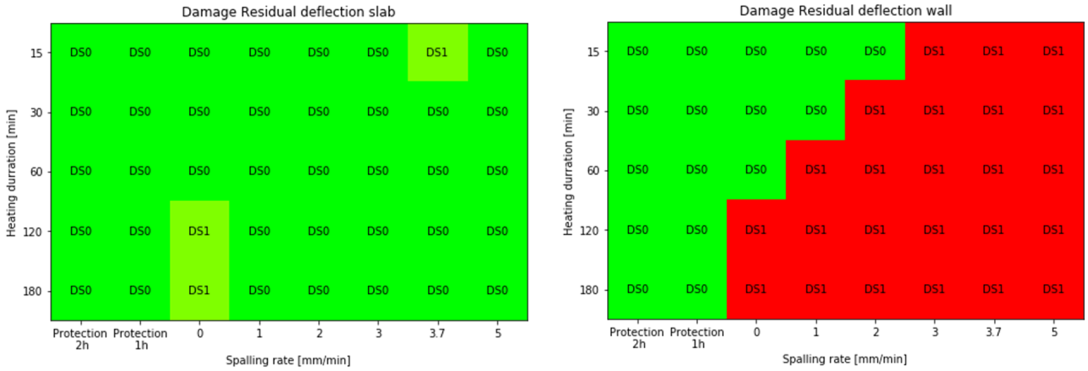

Figure 8. Structural damage state (ceiling and wall) in function of RWS heating phase duration and nominal rate of concrete spalling.

continues to penetrate into the interior of the lining. At 130 minutes the ceiling bottom reinforcement reaches its maximum temperature of approximately 270°C. This maximum temperature is within the range where the reinforcement can be considered to fully recover [6]. Similar results are obtained for the fire-exposed walls. As the concrete cover is larger for the walls, the maximum reinforcement temperature at the exposed side is lower (189°C, attained at approximately 168 minutes). The depth of the 300°C isotherm reaches a maximum around 113 minutes with a depth of 60-65 mm. This result applies to both the ceiling and wall. The thermal damage classification is DS2 both for the ceiling and wall.

The tunnel section withstands the modelled exposure without structural failure. However, the fire exposure does result in permanent deformations and load redistributions. Importantly, to obtain a full view on the structural response, the calculation needs to be continued for beyond the end of the heating phase. In Figure 4, the axial force (top) and bending moment (bottom) in the tunnel section are visualized at the start of the exposure (compression blue, tension yellow colour; bending moment drawn at the tension side). Figure 5 visualizes the same at approximately 60 min, and Figure 6 at 12 hours since the start of the nominal fire exposure. In these figures, displacements are visualized with a factor 10.

The maximum ceiling mid-span deformation is obtained at approximately 115 min since the start of the exposure (approximately 55 mm). The recovery of the deformation takes multiple hours. The residual total mid-span deformation is 36.4 mm. The mechanical damage classification for the ceiling is DS0. The same applies to the wall.

3.2. Damage classification summary

None of the simulated tunnels fail during the fire exposure. The possibility of failure has however been confirmed through simulations with characteristic loading. In the current evaluation, expected values for the load conditions have been considered as indicated in Section 2.1.

Figure 7 and Figure 8 show the matrix plots for the thermal and mechanical damage for different RWS fire duration and nominal spalling rates. The plots also include damage classifications for fire protected structures (i.e. tunnels cladded with passive fire protection boards with a nominal rating of 1h or 2h protection).

Combining the results of Figure 7 and Figure 8 with the spalling probabilities listed in Section 2.3 above, damage class probabilities are obtained in function of the equivalent fire severity (Figure 9 for the ceiling damage classes for unprotected tunnel linings). Figure 9 highlights how also limited fire exposure results in a damage class of at least DS2, and a high proba-

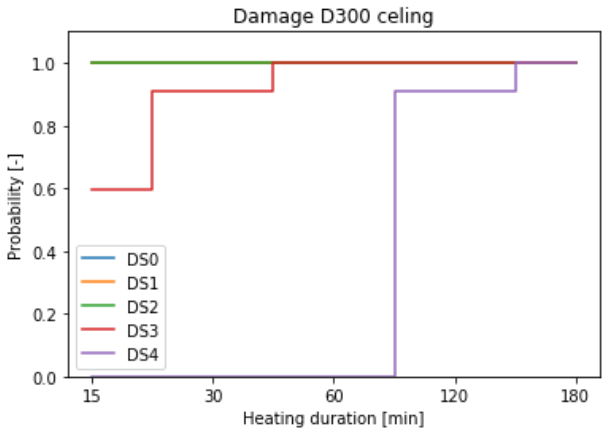

FIGURE 9. Structural damage state probabilities (probability of damage class DSx or higher) for unprotected tunnel ceiling in function of RWS heating phase duration. Note that the damage class is evaluated for the heating durations 15/30/60/120/180 minutes only.

bility of class DS3. Probabilities of DS4 are however observed only from 120 minutes heating duration onwards (note that only a limited number of discrete heating durations are modelled here). The results of Figure 9 are subsequently combined with the RWS heating phase duration probabilities provided by the FESG fire severity model, thus resulting in damage class probabilities for a given tunnel with specific traffic intensity and active/passive fire safety measures. Within the larger risk assessment tool, these damage class probabilities are subsequently translated into assessments of the downtime and repair costs.

4. Conclusions

The structural fire performance of a reference concrete tunnel has been evaluated, taking into account different RWS heating durations and nominal spalling rates. The total simulated time is 12 hours to explicitly evaluate the cooling of the structure. The importance of an explicit evaluation of the cooling phase behaviour has been demonstrated through an example, and the probabilities of achieving set thermal and structural damage states post-fire have been assessed. The results will be incorporated in a simplified risk assessment tool, allowing to compare the risk profile of design alternatives for concrete road tunnels.

Acknowledgements

This study has been made possible through funding from FESG, supported by VLAIO (Flanders Innovation & Entrepreneurship).

5. Bibliography

[1] R. Van Coile, M. Schepers, M. Pachera, M., et al. Risk acceptance framework for specifying fire safety measures in tunnels. *13th International Conference on Structural Safety and Reliability (ICOSSAR 2021)*, 20-24/06 Shanghai, China, 2022.

[2] J.-M. Franssen, T. Gernay. Modeling structures in fire with SAFIR®: theoretical background and capabilities. *Journal of Structural Fire Engineering* **8**(3):300-23, 2017. https://doi.org/10.1108/jsfe-07-2016-0010.

[3] EN 1992-1-2:2004. E*urocode 2: Design of concrete structures - Part 1-2: General rules - Structural fire design*. European standard, 2004. https://www.phd.eng.br/wp-content/uploads/2015/12/en.1992.1.2.2004.pdf.

[4] T. Gernay, J. M. Franssen. A formulation of the Eurocode 2 concrete model at elevated temperature that includes an explicit term for transient creep. *Fire Safety Journal* **51**:1-9, 2012. https://doi.org/10.1016/j.firesaf.2012.02.001.

[5] T. Gernay, A. Millard, J.-M. Franssen. A multiaxial constitutive model for concrete in the fire situation: Theoretical formulation. *International Journal of Solids and Structures* **50**(22-23):3659-73, 2013. https://doi.org/10.1016/j.ijsolstr.2013.07.013.

[6] Fib. *Fire design of concrete structures - structural behaviour and assessment*. fib bulletin 46. The International Federation for Structural Concrete. Lausanne, Switzerland, 2008.

[7] B. Jovanović, R. Van Coile, D. Hopkin, et al. *Review of Current Practice in Probabilistic Structural Fire Engineering: Permanent and Live Load Modelling. Fire Technology* **57**(1):1-30, 2020. https://doi.org/10.1007/s10694-020-01005-w.

[8] A. J. Breunese, C. Both, G. M. Wolsink, G.M. *Fire testing procedure for concrete tunnel linings*. TNO-rapport 2008-Efectis-R0695, Bleiswijk, the Netherlands, 2008.

[9] H. Ingason, S. Gustavsson, M. Dahlberg. *Heat release rate measurements in tunnel fires*. Brandforsk project 723-924 (SP Report 1994:08). Swedish National Testing and Research Institute, Boras, Sweden, 1994.

[10] Fib. *Performance-based design of concrete structures (committee draft 2021-06-24)*. The International Federation for Structural Concrete. Lausanne, Switzerland, 202.

[11] N. Hua, A. Tessari, N. Elhami Khorasani. Characterizing damage to a concrete liner during a tunnel fire. *Tunnelling and Underground Space Technology* **109**, 2021. https://doi.org/10.1016/j.tust.2020.103761.

[12] T.G. Van der Waart van Gulik, A. J. Breunese, R. Jansson, R., et al. Spalling behaviour of a non-spalling qualified concrete. *4th International Workshop on Concrete Spalling due to Fire Exposure*, 08-09/10 Leipzig, Germany, 2015.

[13] C. Maluk, L. Bisby, G. P. Terrasi. Effects of polypropylene fibre type and dose on the propensity for heat-induced concrete spalling. *Engineering Structures* **141**:584-95, 2017. https://doi.org/10.1016/j.engstruct.2017.03.058.

[14] H. Akaike. A new look at the statistical model identification. *IEEE Transactions on Automatic Control* **19**(6):716-23, 1974. https://doi.org/10.1109/tac.1974.1100705.

[15] S. Ni, T. Gernay. A framework for probabilistic fire loss estimation in concrete building structures. *Structural Safety* **88**, 2021. https://doi.org/10.1016/j.strusafe.2020.102029.